Biomass characterization and biogas production of pretreated straw: is there a correlation?

Vincenzo Calcagno[1,2], Shruthi Meenakshisundaram[1], Claire Ceballos[1], Antoine Fayeulle[1], Estelle Leonard[1], Virginie Herledan[2], Jean-Marc Kraft[2], Yannick Millot[2], Xiaojun Liu[1], Claude Jolivalt[2], André Pauss[1]

[1]Université de technologie de Compiègne, ESCOM, TIMR (Integrated Transformations of Renewable Matter), Centre de recherche Royallieu - CS 60 319, F-60 203 Compiègne Cedex, France
[2]Sorbonne Université, CNRS, Laboratoire de Réactivité de Surface, 4 place Jussieu, 75005 Paris, France
vincenzo.calcagno@utc.fr

Abstract – Lignocellulosic biomass is a very attractive substrate for biogas production via anaerobic digestion. Among all, straw represents a very interesting and worldwide diffused agricultural by-product. However, due to the intrinsically complex structure of lignocellulosic biomass, straw has low biodegradability which results in low biogas yield. To increase the biogas production, chemical and physical pretreatments have been performed – i.e., size reduction, autoclave, and oxidation. The pretreatment conditions have been mitigated, in order to reduce their economic impact on the overall process and to make such pretreatments attractive at industrial level.

The effects of the biomass pretreatments have been evaluated both by assessing the biomethane productivity in an anaerobic bioreactor and, in parallel, by characterizing the biomass at different levels – elemental content, functional groups, structural changes, and surface morphology. Results show a poor correlation between biogas production and the structural and chemical biomass changes. These findings confirm a more general issue: the difficulty of using biomass characterization alone to explain and predict the biogas production enhancement and of using such information to further improve biomass pretreatments.

Keywords: anaerobic digestion; biomass; straw pretreatment; size reduction; autoclave; Fenton reaction.

I. Introduction

Lignocellulosic biomass (LCB), as the name suggests, refers to plant-based raw materials containing three main polymers called cellulose, hemicellulose, and lignin.[1] Due to its abundance, LCB provides an interesting resource for sustainable fuels production. Biogas composed of biomethane and carbon dioxide, one of the renewable energy vectors, can be produced from LCB through anaerobic digestion (AD). AD is realized by a consortium of microorganisms which transform the biodegradable organic matter into biomethane. At the same time, being a composite of three very different and intertwined components, it results to be recalcitrant to any biological degradation or traditional separation process. Consequently, a key challenge to render LCB even more attractive at industrial level is to increase its biofuels yield. To this aim, a pretreatment step, or a combination of pretreatments, can be applied to increase the biofuel yield [1, 2]. Of course, reducing the pretreatment costs enough can make LCB even more competitive in price with fossil-derived fuels.

Among the available source of LCB, straw represents a substantial agricultural by-product around the world, making it an attractive substrate for biogas production.

In this talk the effect of chemical and physical pretreatments are presented. In particular, size reduction, autoclaving and chemical oxidation of straw have been performed as a combined pretreatment. The use of a combination of pretreatments helps to conduct the individual steps at milder conditions, thus reducing the overall economic and environmental impact. [3, 4] The effect of the pretreatment has been evaluated both in terms of biomethane production and in terms of structural and chemical biomass changes.

II. Results

The ground and sieved straw was separated into two size fractions (0.63 – 2 mm and 2.5 – 4 mm, respectively) and accordingly pretreated by autoclave (121°C, 1 bar, 20 minutes) and Fenton reaction [5]. On the pretreated samples and the controls for each pretreatment, BMP measurement and biomass characterization using a range of techniques were carried out.

A. Biochemical Methane Potential

Biochemical Methane Potential (BMP) were performed using an automatic methane potential test system (AMPTS II, Bioprocess, Lund, Sweden) that measures the biomethane obtained from the anaerobic digestion of biodegradable substrates. The AD of the straw, pretreated or not, was carried

out in triplicate in mesophilic condition (37 °C) using an inoculum treating energy cultures.

The total cumulative methane yield, after 57 days for all samples (Figure 1) is significantly higher for the small-size fraction straw whatever the other pretreatments as compared to the large-size fraction straw. Moreover, autoclaving does not significantly improve the cumulative methane yield. Interestingly, the Fenton pretreatment, carried out with very low concentrations of oxidizing agent (1.047 mM of Fe^{2+} and 0.1475 M of H_2O_2), does not significantly influence alone the cumulative biomethane yield, but when the biomass was autoclaved and then followed by Fenton pretreatment, the cumulative biomethane increase was 10.9% and 17.0%, respectively for small and large-size fraction straws. Overall, the combination of particle size reduction, autoclaving and Fenton reaction produced the highest methane potential (356 ± 11 NL_{CH4}/kg VS). Therefore, the synergy of combined pretreatments is better than single pretreatments.

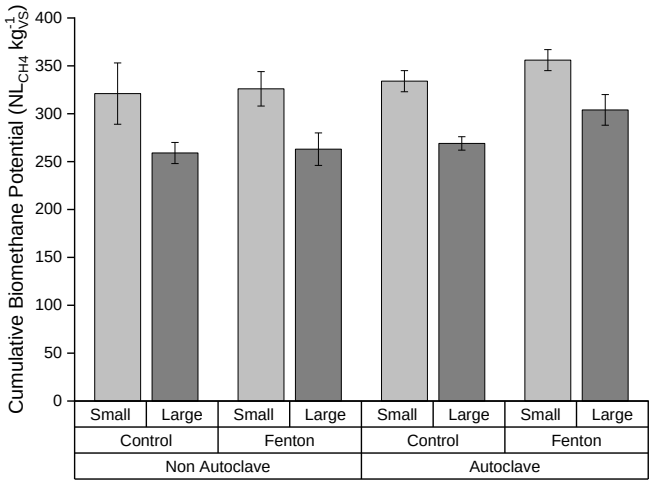

Figure 1. Total cumulative methane yield after 57 days

B. *Structural and chemical characterizations*

1) *Compositional analysis*

Elemental composition (carbon C, hydrogen H, nitrogen N, sulfur S, and oxygen O contents) was determined for all the straw samples (Table 1).

Table 1. Elemental composition (C, H, N, S, O) of control and Fenton pretreated (C and F, respectively in the sample name), autoclaved and not (A and NA, respectively in the sample name) straw for both small and large-size particles (S and L, respectively in the sample name).

Sample	***% C***	***% H***	***% N***	***% S***	***% O***
S-NA-C	44.7 ± 0.5	5.8 ± 0.0	0.3 ± 0.0	0.3 ± 0.5	40.4 ± 0.1
S-NA-F	44.7 ± 0.6	5.7 ± 0.0	0.3 ± 0.0	0.1 ± 0.1	42.7 ± 0.2
S-A-C	45.1 ± 1.1	5.7 ± 0.1	0.3 ± 0.0	0.4 ± 0.3	43.6 ± 0.5
S-A-F	43.6 ± 0.6	5.5 ± 0.1	0.3 ± 0.0	0.0 ± 0.0	44.2 ± 0.2
L-NA-C	44.8 ± 0.1	5.7 ± 0.1	0.2 ± 0.1	0.2 ± 0.2	40.1 ± 0.1
L-NA-F	44.3 ± 0.5	5.6 ± 0.0	0.2 ± 0.1	0.0 ± 0.0	43.0 ± 0.9
L-A-C	45.1 ± 1.2	5.7 ± 0.1	0.2 ± 0.1	0.0 ± 0.0	39.6 ± 0.8
L-A-F	44.2 ± 0.4	5.6 ± 0.1	0.4 ± 0.3	0.3 ± 0.3	43.6 ± 0.6

Moreover, the lignin composition (acid-soluble fraction of lignin ASL, and acid-insoluble lignin AIL) analysis [6] was also determined (Figure 2).

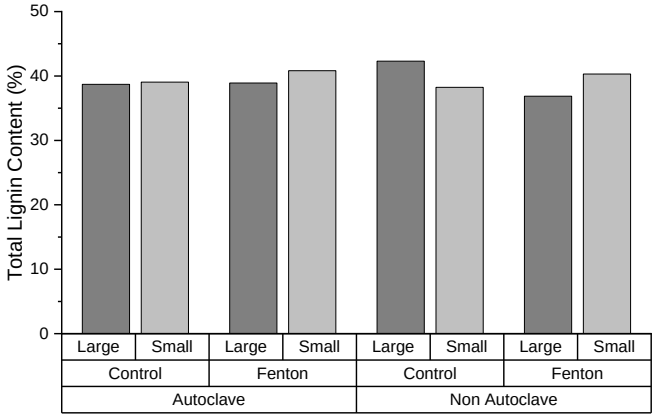

Figure 2. Total lignin content (%) as a sum of acid-soluble (ASL) and acid-insoluble (AIL) fractions in pre-treated samples as compared to their corresponding controls.

While no great differences are observed in the elemental composition of the straw after pretreatments, the proportion of lignin has different trends in the case of large- or small-size particle samples. For small-size particles lignin content is enhanced after both autoclave and Fenton reaction pretreatment. This could be due to the lignification of silica bodies [7] and/or the presence of lignin in stomatal cell walls [8]. On the other side, for large-size no autoclaved straw lignin degradation due to the different pretreatment conditions is observed. Nevertheless, higher lignin degradation does not always translate into a higher percentage of BMP enhancement, as confirmed from the comparison with the BMP results.

2) *Porosity indicator by Simons' Staining*

Simons' staining test is an interesting method used to evaluate any structural variation occurring in biomass ultrastructure upon pretreatment. With this test, it is possible to evaluate the variation in the pore size distribution of the lignocellulosic samples [9, 10]. This would be an interesting parameter

characterizing the accessibility of degradable substrates (cellulose and hemicellulose) to the microorganisms. Accordingly, pretreated straw samples and the related controls have been analyzed to assess any change in the porosity. Results (Figure 3) indicate that the Fenton reaction produces a significant increase in porosity, but the method does not point out any relevant differences between autoclaved and not autoclaved samples. A slightly higher porosity can be seen for the larger size, but such difference is not statistically relevant, as confirmed by ANOVA test.

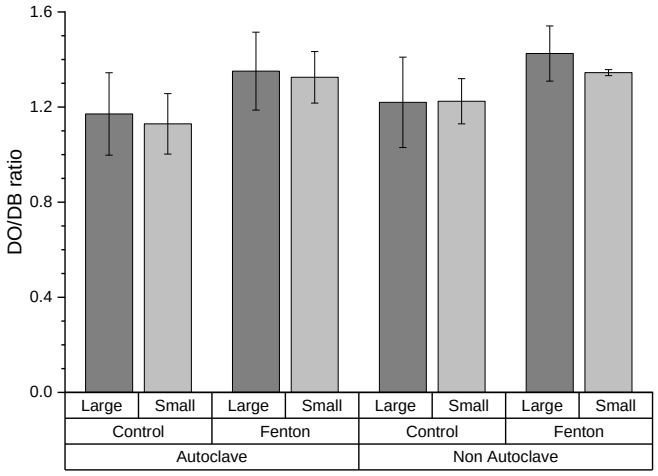

Figure 3. Porosity indication for control and pretreated straw obtained using Simon's staining technique

3) *Infrared spectroscopy and second derivative analysis*

In Figure 4 are shown the normalized ATR spectra in the fingerprint region obtained for all the samples.

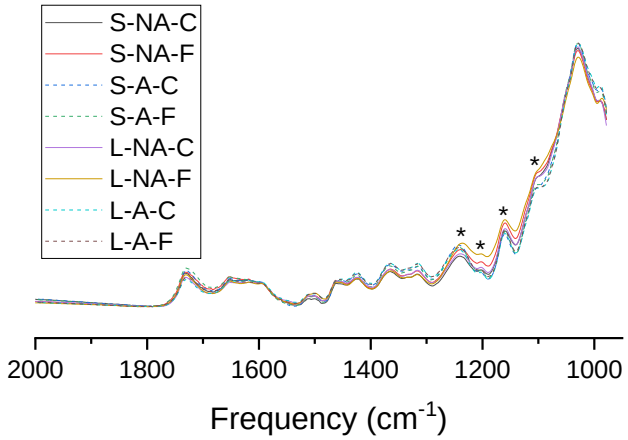

Figure 4. ATR spectra of controlled and pretreated samples in the fingerprint region. The resulting bands modified upon autoclave are indicated with a star (*). The samples subjected to autoclaving are indicated with dotted lines.

At first sight, no obvious modifications in the FTIR data after the pretreatment are observed. However, based on the differences resulting from the second derivative analysis, some difference become visible the fingerprint region in the range of 1300-1050 cm^{-1} (Figure 5). Based on such differences, spectra can be separated into two groups, depending on whether they were autoclaved or not. Namely, the bands at 1235 cm^{-1} and 1200 cm^{-1}, both related to the OH out-of-plane vibration mode of cellulose [11], are broadened and shifted at lower frequencies for samples not subjected to autoclave. Also, the band at 1160 cm^{-1}, related to the antisymmetric bridge stretching of C-O-C of cellulose and hemicellulose [12], is sharper after the autoclaved samples. Lastly, the intensity of the band at 1100 cm^{-1}, related to the amorphous cellulose [12, 13], was reduced after the autoclave. These data suggest that slight, also significant, differences in the cellulose and/or hemicellulose can be evidenced by second derivative ATR-FTIR spectra after autoclave

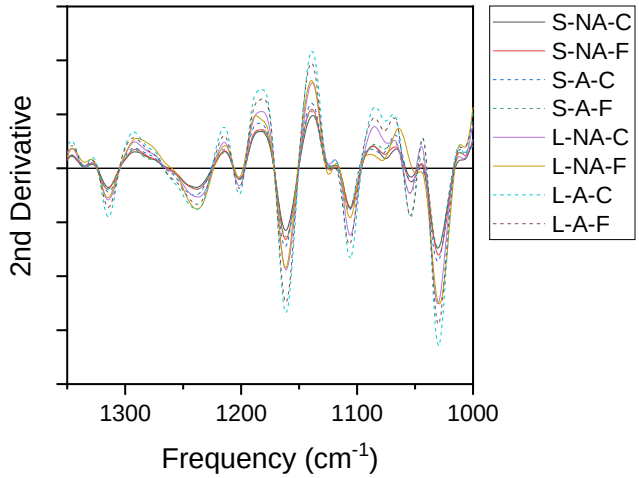

Figure 5. Second derivative analysis of ATR spectra in the range between 1350 cm^{-1} and 1000 cm^{-1}. The samples subjected to autoclaving are indicated with dotted lines.

4) *Cellulose crystallinity and lateral fibril size*

The cellulose crystallinity (Crystallinity Index, CI) which is an estimation of the relative amounts of crystalline (ordered) and amorphous (less ordered) part of the biomass is a key parameter often used to characterize the biomass after pretreatment [14]. Among the techniques used to estimate crystalline index, solid-state ^{13}C NMR (ssNMR) was reported to be very powerful [15]. The results from NMR analysis are shown in Figure 6 and they show that the cellulose CI remain approximately constant for all samples (around 40%). In addition to the CI calculation, NMR analysis is also useful to estimate the supramolecular structures of cellulose [17, 18].

Indeed, cellulose is structured in fibrils with a crystalline core surrounded by a non-crystalline cellulose layer. In turn, cellulose fibrils aggregate in microfibrils, or fibril bundles, so that only a fraction of the non-crystalline cellulose is accessible to the solvent: any change in the cellulose fibril dimension (Lateral Fibril Dimension, LFD) and microfibril dimension (Lateral Fibril Aggregate Dimension, LFAD) can influence the biomethane production. The results from NMR analysis (Figure 7) indicate that pretreatment conditions have no significant effects on the supramolecular structures of cellulose.

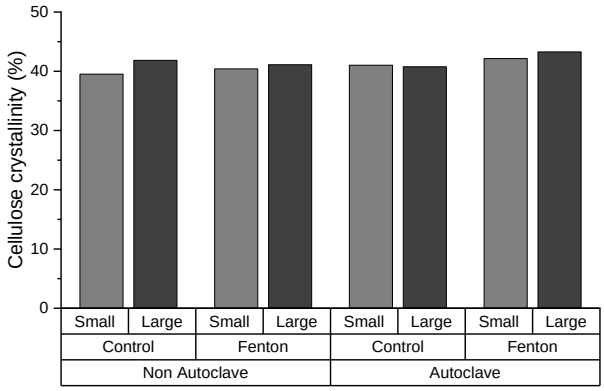

Figure 6. Cellulose crystallinity obtained by NMR analysis of the pretreated samples.

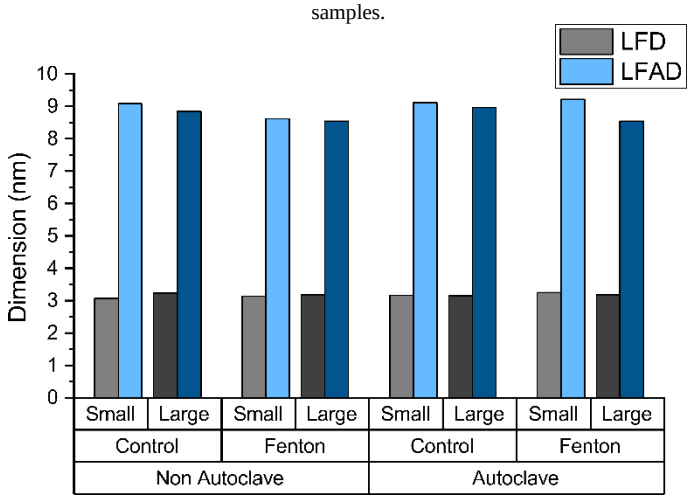

Figure 7. Lateral Fibril Dimension (LFD) and Lateral Fibril Aggregate Dimension (LFAD) for the different samples as determined by NMR analysis.

III. Conclusion and Perspectives

The synergy of combined pretreatment, namely particle size reduction, autoclaving and Fenton reaction produced the highest methane potential (356 ± 11 NL_{CH4}/kg_{VS}). The intricacy of the lignocellulosic matrix and heterogeneity in physicochemical composition within the species makes it complex to study and to find a biomass characterization and biogas production. Results show that the conventional biomass characterization alone is not sufficient to explain the effect of pretreatment on biogas production and, even more, to indicate what kind of modifications should be targeted by the pretreatment to obtain an improvement of biogas yield. Without further improvement and development of analytical techniques, the explanation and the prediction of the biomethane potential of a feedstock with the aid of pretreatment can only be considered in case-by-case studies.

References

[1] Sun, L.; Müller, B.; Schnürer, A. Biogas Production from Wheat Straw: Community Structure of Cellulose-Degrading Bacteria. *Energy Sustain. Soc.* **2013**, *3*, 15, doi:10.1186/2192-0567-3-15.

[2] Baruah, J.; Nath, B.K.; Sharma, R.; Kumar, S.; Deka, R.C.; Baruah, D.C.; Kalita, E. Recent Trends in the Pretreatment of Lignocellulosic Biomass for Value-Added Products. *Front. Energy Res.* **2018**, *6*, 141, doi:10.3389/fenrg.2018.00141.

[3] Kumar, A.K.; Sharma, S. Recent Updates on Different Methods of Pretreatment of Lignocellulosic Feedstocks: A Review. *Bioresour. Bioprocess.* **2017**, *4*, 7, doi:10.1186/s40643-017-0137-9.

[4] Meenakshisundaram, S.; Fayeulle, A.; Leonard, E.; Ceballos, C.; Pauss, A. Fiber Degradation and Carbohydrate Production by Combined Biological and Chemical/Physicochemical Pretreatment Methods of Lignocellulosic Biomass – A Review. Bioresour. Technol. 2021, 331, 125053, doi:10.1016/j.biortech.2021.125053.

[5] Kato, D.M.; Elía, N.; Flythe, M.; Lynn, B.C. Pretreatment of Lignocellulosic Biomass Using Fenton Chemistry. *Bioresour. Technol.* **2014**, *162*, 273–278, doi:10.1016/j.biortech.2014.03.151.

[6] Sluiter, A.; Hames, B.; Ruiz, R.; Scarlata, C.; Sluiter, J.; Templeton, D.; Crocker, D. *Determination of Structural Carbohydrates and Lignin in Biomass*; 2012.

[7] Guerriero, G.; Hausman, J.-F.; Legay, S. Silicon and the Plant Extracellular Matrix. *Front. Plant Sci.* **2016**, *7*, doi:10.3389/fpls.2016.00463.

[8] Shtein, I.; Shelef, Y.; Marom, Z.; Zelinger, E.; Schwartz, A.; Popper, Z.A.; Bar-On, B.; Harpaz-Saad, S. Stomatal Cell Wall Composition: Distinctive Structural Patterns Associated with Different Phylogenetic Groups. *Ann. Bot.* **2017**, *119*, 1021–1033, doi:10.1093/aob/mcw275.

[9] Simons, F.L. A Stain for Use in the Microscopy of Beaten Fibers. *Tappi* **1950**, *33*, 312–314.

[10] Chandra, R.; Ewanick, S.; Hsieh, C.; Saddler, J.N. The Characterization of Pretreated Lignocellulosic Substrates Prior to Enzymatic Hydrolysis, Part 1: A Modified Simons' Staining Technique. *Biotechnol. Prog.* **2008**, *24*, 1178–1185, doi:10.1002/btpr.33.

[11] Schwanninger, M.; Rodrigues, J.C.; Pereira, H.; Hinterstoisser, B. Effects of Short-Time Vibratory Ball Milling on the Shape of FT-IR Spectra of Wood and Cellulose. *Vib. Spectrosc.* **2004**, *36*, 23–40, doi:10.1016/j.vibspec.2004.02.003

[12] Stewart, D.; Wilson, H.M.; Hendra, P.J.; Morrison, I.M. Fourier-Transform Infrared and Raman Spectroscopic Study of Biochemical and

Chemical Treatments of Oak Wood (Quercus Rubra) and Barley (Hordeum Vulgare) Straw. *J. Agric. Food Chem.* **1995**, *43*, 2219–2225, doi:10.1021/jf00056a047.

[13] Nelson, M.L.; O'Connor, R.T. Relation of Certain Infrared Bands to Cellulose Crystallinity and Crystal Latticed Type. Part I. Spectra of Lattice Types I, II, III and of Amorphous Cellulose. *J. Appl. Polym. Sci.* **1964**, *8*, 1311–1324, doi:10.1002/app.1964.070080322.

[14] Park, S.; Baker, J.O.; Himmel, M.E.; Parilla, P.A.; Johnson, D.K. Cellulose Crystallinity Index: Measurement Techniques and Their Impact on Interpreting Cellulase Performance. **2010**, 10.

[15] Bernardinelli, O.D.; Lima, M.A.; Rezende, C.A.; Polikarpov, I.; deAzevedo, E.R. Quantitative 13C MultiCP Solid-State NMR as a Tool for Evaluation of Cellulose Crystallinity Index Measured Directly inside Sugarcane Biomass. *Biotechnol. Biofuels* **2015**, *8*, 110, doi:10.1186/s13068-015-0292-1.

[16] Wickholm, K.; Larsson, P.T.; Iversen, T. Assignment of Non-Crystalline Forms in Cellulose I by CP/MAS 13C NMR Spectroscopy. *Carbohydr. Res.* **1998**, *312*, 123–129, doi:10.1016/S0008-6215(98)00236-5.

[17] Zuckerstätter, G.; Terinte, N.; Sixta, H.; Schuster, K.C. Novel Insight into Cellulose Supramolecular Structure through 13C CP-MAS NMR Spectroscopy and Paramagnetic Relaxation Enhancement. *Carbohydr. Polym.* **2013**, *93*, 122–128, doi:10.1016/j.carbpol.2012.05.019.

[18] Chunilall, V.; Bush, T.; Larsson, P.T.; Iversen, T.; Kindness, A. A CP/MAS 13C-NMR Study of Cellulose Fibril Aggregation in Eucalyptus Dissolving Pulps during Drying and the Correlation between Aggregate Dimensions and Chemical Reactivity. *Holzforschung* **2010**, *64*, doi:10.1515/hf.2010.097.